Redox Biology 53 (2022) 102339

Contents lists available at ScienceDirect

Redox Biology

journal homepage: www.elsevier.com/locate/redox

ROS generation attenuates the anti-cancer effect of CPX on cervical cancer cells by inducing autophagy and inhibiting glycophagy

Hui Fan [a,1], Yujia He [b,c,1], Junqi Xiang [a], Jing Zhou [c], Xinyan Wan [a], Jiawei You [d], Kailong Du [a], Yue Li [a], Lin Cui [a], Yitao Wang [a], Chundong Zhang [a], Youquan Bu [a], Yunlong Lei [a,*]

[a] Department of Biochemistry and Molecular Biology, and Molecular Medicine and Cancer Research Center, College of Basic Medical Sciences, Chongqing Medical University, Chongqing, 400016, China
[b] Department of Laboratory Medicine, Sichuan Provincial People's Hospital, University of Electronic Science and Technology of China, 610041, PR China
[c] State Key Laboratory of Biotherapy and Cancer Center, West China Hospital, and West China School of Basic Medical Sciences & Forensic Medicine, Sichuan University, and Collaborative Innovation Center for Biotherapy, Chengdu, 610041, PR China
[d] Department of Basic Medicine, and Molecular Medicine and Cancer Research Center, College of Basic Medical Sciences, Chongqing Medical University, Chongqing, 400016, China

ARTICLE INFO

Keywords:
CPX
Cervical cancer
Glycophagy
PARK7/DJ-1
ROS

ABSTRACT

Cervical cancer is one of the most common gynecological malignancies with poor prognosis due to constant chemoresistance and repeated relapse. Ciclopirox olamine (CPX), a synthetic antifungal agent, has recently been identified to be a promising anti-cancer candidate. However, the detailed mechanisms related to its anti-cancer effects remain unclear and need to be further elucidated. In this study, we found that CPX could induce proliferation inhibition in cervical cancer cells by targeting PARK7. Further results demonstrated that CPX could induce cytoprotective autophagy by downregulating the expression of PARK7 to activate PRKAA1 or by PARK7-independent accumulation of ROS to inhibit mTOR signaling. Meanwhile, CPX treatment increased the glycogen clustering and glycophagy in cervical cancer cells. The presence of N-acetyl-L-cysteine (NAC), a ROS scavenger, led to further clustering of glycogen in cells by reducing autophagy and enhancing glycophagy, which promoted CPX-induced inhibition of cervical cancer cell proliferation. Together, our study provides new insights into the molecular mechanisms of CPX in the anti-cancer therapy and opens new avenues for the glycophagy in cancer therapeutics.

1. Introduction

Cervical cancer is one of the most common cancers in women, and its morbidity and mortality rank fourth among female malignancies. In 2020, about 604,000 cases and 342,000 deaths of cervical cancer were reported worldwide and the morbidity and mortality in China accounted for 18% and 17%, respectively [1,2]. The incidence of cervical cancer has been on the rise in recent years, especially among young adult women. Standard treatments for cervical cancer include surgery, chemotherapy, and radiotherapy. Despite recent advances, the long-term prognosis of cervical cancer remains poor because of resistance and recurrence [3]. Consequently, there is an urgent need to develop novel targeted therapeutic agents for cervical cancer to improve the survival rates.

Ciclopirox olamine (CPX) is a synthetic antifungal agent and iron chelator that has been used to treat the mycoses of the skin and nails for decades. Recent preclinical and clinical studies have shown that CPX also possesses promising anti-cancer activities [4–6]. Our previous study has demonstrated the anti-colorectal cancer effects of CPX by inducing cell apoptosis and inhibiting cell proliferation, which is mediated by the down-regulation of PARK7 and the accumulation of ROS [5]. In addition, CPX can also exert its anti-cancer activity by suppressing cell migration and invasion [7]. Notably, pharmacological and toxicological profiles from preclinical and clinical studies support that systemic administration of CPX is feasible and safe for cancer treatment [8]. However, the detailed molecular mechanisms of CPX in cervical cancer remain to be further elucidated.

* Corresponding author. Department of Biochemistry and Molecular Biology, and Molecular Medicine and Cancer Research Center, College of Basic Medical Sciences, Chongqing Medical University, Chongqing, 400016, PR China.
E-mail address: leiyunglong@cqmu.edu.cn (Y. Lei).
[1] These authors contributed equally to this work.

https://doi.org/10.1016/j.redox.2022.102339
Received 2 April 2022; Received in revised form 8 May 2022; Accepted 12 May 2022
Available online 17 May 2022

Abbreviations

ATG5	autophagy related 5
CPX	Ciclopirox olamine
CQ	chloroquine
GABARAPL1	GABA type A receptor associated protein like 1
GYS1	glycogen synthase 1
GSK3B	glycogen synthase kinase 3 beta
LDH	lactate dehydrogenase
MAP1LC3B/LC3B	microtubule associated protein 1 light chain 3 beta
mTOR	mechanistic target of rapamycin kinase
NAC	N-acetyl-L-cysteine
PARK7/DJ-1	Parkinsonism associated deglycase
PRKAA1/AMPK	AMP-activated protein kinase
PYGL	glycogen phosphorylase L
ROS	reactive oxygen species
RPS6KB1/p70S6K	ribosomal protein S6 kinase B1
SQSTM1/p62	sequestosome 1
STBD1	starch binding domain 1
YAP1	Yes1 associated transcriptional regulator

PARK7, a member of the PARK7/ThiJ/PfpI protein superfamily, is a pathogenic gene for familial Parkinson's disease [9,10], and is generally recognized as an oxidative stress sensor with antioxidant and neuroprotective effects [11]. Increasing evidence suggested that PARK7 also plays a critical role in tumor development and progression [12]. PARK7 has been identified as a prognostic marker for patients with colorectal cancer, liver cancer, and pancreatic cancer. Patients with high PARK7 expression often have a poor prognosis [13–15]. Thus, it is interesting to explore the functional role of PARK7 in cervical cancer.

Autophagy is a lysosome-dependent catabolic pathway by which damaged or senescent organelles are removed. Autophagy plays an important role in the regulation of cancer progression and in determining the response of tumor cells to stress induced by chemotherapy. However, the role of autophagy in cancer therapy is multifaceted, depending on the cell type, microenvironment and the stage of tumor development [16–18]. Cytoprotective and cytotoxic functional forms of autophagy have been described to date, of which cytoprotective autophagy is more frequent in response to chemotherapy. A series of evidence implicated that autophagy can enhance the acquired resistance of cancer cells during chemotherapy, resulting in the limited effectiveness of many anti-cancer drugs, which suggests that autophagy could be a potential target for cancer treatment [19–21]. Up to know, more than 20 different types of selective autophagy have been found according to different types of cytoplasmic contents, such as glycophagy, mitophagy and lysophagy [22]. A recent study reported the involvement of glycophagy in cancer regulation, which further indicates that aberrant autophagy selectivity is highly correlated with human cancers. STBD1, the adaptor protein which targets glycogen particles for their degradation through glycophagy, inhibits tumor growth via modulating glycophagy and inhibiting the metabolic reprogramming in cancer cells [23]. These findings open new avenues of selectively targeted autophagy for cancer therapeutics.

As the largest macromolecule in the cytosol, glycogen is stored primarily in the liver and muscle cells for energy reserves in mammals [24]. Synthesis and breakdown of glycogen is mainly accomplished by glycogen synthase (GYS1) and glycogen phosphorylase (PYGL). Loss-of-function mutations in glycogenolysis enzymes lead to glycogen storage diseases (GSDs), marked hepatomegaly, and development of hepatocellular adenomas and carcinomas [24–26]. Glycogen metabolism is closely related to tumor aggressiveness and the survival of cancer cells [27]. The accumulation of glycogen has been reported to block the activities of Hippo signal and consequently activates YAP1, which promotes liver enlargement and cancer development [28]. Several studies also showed that glycogen is accumulated to improve several types of tumor cell survival under hypoxia or other stress conditions [29–31]. In addition, glycogen has been reported to be a sensitive indicator of the responsiveness of cervical cancer to treatment and no glycogen clustering was observed in patient cells with a poor response to chemotherapy [32].

In this study, we found that CPX inhibited the proliferation of cervical cancer cells by targeting PARK7. CPX also induces cytoprotective autophagy through PARK7-induced activation of PRKAA1 and PARK7-independent accumulation of ROS. Notably, we found the important role of ROS in the regulation of glycogen clusters, glycophagy and inactivation of YAP1 and their involvement in CPX-treated cervical cancer cells.

2. Materials and methods

2.1. Cell culture

Human cervical cancer cell lines HeLa and SiHa were obtained from the American Type Culture Collection (ATCC). Cells were routinely maintained in DMEM (Hyclone, Utah, USA) and MEM (Hyclone) medium supplemented with 10% of fetal bovine serum (Hyclone), penicillin (10^7 U/L) and streptomycin (10 mg/L) in a humidified incubator containing 5% CO_2 at 37 °C. The last time of authentication for these cells was November 2021.

2.2. Antibodies and reagents

Antibodies were shown in Supplementary Table 1.

Ciclopirox olamine (1134030), E64D (E8640) and PepA (P5318) were purchased from Sigma. Bafilomycin A1 (HY-100558), CQ (HY-17589A), Compound C (HY-13418), Wortmannin (HY-10197), Cycloheximide (HY-12320) were purchased from MedChemExpress. NAC (Beyotime, ST1546).

2.3. Cell viability and proliferation assays

CCK8 assay was performed to determine the cell viability. Briefly, cells were seeded in 96-well plates at a density of 4000 cells. After treatment, CCK8 (Bimake, B34302) reagents were added and incubated for 1h. The absorbance value was then determined at 450 nm.

The long-term effects of CPX on cervical cancer cell proliferation were analyzed with colony formation assays. After treatment, 800–1000 cells were seeded in twelve-well plates and the medium was changed every 3 days. After two weeks, cells were fixed with 4% paraformaldehyde (Sigma) for 30 min and stained with Crystal Violet for another 30 min, and then the colonies were washed three times and taken photos.

2.4. Immunoblotting and immunoprecipitation

Cells were lysed with RIPA buffer (Beyotime) supplemented with protease inhibitor cocktail (Sigma) and then protein lysates were centrifuged and boiled with loading buffer. For immunoprecipitations, cells were lysed with IP lysis buffer (Beyotime) and incubated with 1 μg of antibody overnight at 4 °C. Next day, Sepharose protein A/protein G beads were added for 2 h. The immune-complexes were then centrifuged and washed 3 times using RIPA buffer. All lysates were quantified by the BCA Protein Assay (Thermo Fisher Scientific) and analyzed by SDS–PAGE.

2.5. Immunofluorescence

Cells grown on coverslips that treated with CPX for 24 h were fixed

with 4% paraformaldehyde (Sigma) for 30 min and then washed three times with PBS. Fixed cells were permeabilized with 0.5% Triton 100 for 20 min and blocked with 1% BSA for 2 h at 37 °C. For staining, cells were incubated with primary antibodies for 12 h at 4 °C, followed by incubation with secondary antibodies (Thermo Scientific) for 1 h at 37 °C. Finally, nuclei were stained with DAPI for 10 min. For autophagy flux studies, cells were transfected with GFP-RFP-LC3 for 24 h and then treated with CPX for another 24 h. Images were captured using a confocal microscopy (Leica).

2.6. Quantitative RT-PCR (qRT-PCR)

Total RNA was extracted using Trizol reagent (Invitrogen) and reverse transcribed using Reverse Transcription PrimeScript 1st Stand cDNA Synthesis kit (TaKaRa, Otsu, Japan). qRT-PCRs were performed using quantitative PCR reagents SYBR PremixEx TaqTM (TaKaRa) following the manufacturer's instructions. Levels of GAPDH quantified with target genes acts as an internal control and fold-changes were analyzed using the $2^{-\Delta\Delta Ct}$ method. The qRT-PCR primer sequences were shown in Supplementary Table 2.

2.7. Transfection

All siRNAs were designed using BLOCK-iT™ RNAi Designer (Invitrogen) and synthesized by GenePharma (Shanghai, China). The sequences of the siRNAs used are listed in Supplementary Table 2. Cells were transfected with siRNAs using Lipofectamine RNAiMax (Invitrogen) according to the manufacturer's instruction. Cells were collected and subjected to subsequent analysis 24h–72h after transfection.

pCMV-myc-PARK7 plasmids were obtained as described previously [33,34]. The plasmids were transfected into the indicated cells using Lipofectamine 3000 (Invitrogen) according to the manufacturer's instruction.

2.8. Cell cycle and apoptosis analysis

Cell cycle distribution was determined by flow cytometry after staining cells with propidium iodide. In brief, floating and adherent cells were collected, washed with ice-cold phosphate-buffered saline (PBS), and fixed with 70% ethanol. The cells were then treated with 50 μg/ml of RNase A and 50 μg/ml of propidium iodide for 30 min at room temperature. The stained cells were analyzed using FACScan flow cytometer (BD Biosciences).

For apoptosis analysis, cells were stained with Annexin V-FITC and propidium iodide using the Annexin V-FITC Apoptosis Detection Kit (Sigma, Saint Louis, USA) and then subjected to FACS analysis.

2.9. Transmission electron microscopy

Transmission electron microscopy assay was used to visualize the autophagic vesicles. After 24-h CPX treatment, HeLa and SiHa cells were fixed in glutaraldehyde (Sigma) and ultrathin sections were prepared using a sorvall MT5000 microtome. Then, the sections were stained by lead citrate and/or 1% uranyl acetate and visualized by Philips EM420 electron microscopy.

2.10. Glycogen staining

Glycogen was detected with a standardized periodic acid Schiff (PAS) staining technique (Solarbio, G1360). Briefly, cervical cancer cells were fixed with PAS Fixative for 10–15 min and then washed with water. Fixed cells were treated with Oxidant at room temperature for 15–20 min. After washing with water, cells were bathed with Schiff's reagent for 15 min in dark place at RT. After rinsing with running water, cells were counterstained with Mayer Hematoxylin Staining Solution. The PAS staining intensity from the image was quantified using ImageJ software.

2.11. Data analysis and statistics

Data were expressed as means ± s.d. All experiments were performed at least three times. Statistical analysis was performed with GraphPad Prism 8.0 software. Statistical differences between groups were determined using two-tailed Student's t-test. Significance was designated as follows: *, $P < 0.05$, **, $P < 0.01$, ***, $P < 0.001$.

3. Results

3.1. CPX inhibits proliferation in cervical cancer cells

To identify whether CPX exhibited the anti-tumor effects against cervical cancer cells, CCK8 assays were applied to assess the cell viability in response to CPX treatment in cervical cancer cells (HPV18-positive HeLa and HPV16-positive SiHa). As shown in Fig. 1A, CPX treatment reduced the cell viability of cervical cancer cells to a certain extent. CCK8 growth curve assays demonstrated that CPX treatment inhibited cervical cancer cell proliferation in a concentration-dependent manner (Fig. S1A). Furthermore, a significant decrease in colony numbers was observed in cervical cancer cells after CPX treatment (Fig. 1B–C). Consistently, the proliferation of cervical cancer cells was markedly inhibited under CPX treatment, as evidenced by reduced EdU incorporation (Fig. 1D–E). Cell cycle analysis revealed that CPX treatment resulted in a remarkable G1 arrest in cervical cancer cells (Fig. S1B). Then we performed lactate dehydrogenase (LDH) assays to determine the cytotoxicity of the drug. CPX treatment caused weak cytotoxicity in HeLa and SiHa cells (Fig. S1C). In addition, Annexin V/PI stainings by flow cytometry further confirmed that CPX had no pro-apoptotic effect in HeLa and SiHa cells (Fig. S1D). In summary, these data indicate that proliferation inhibition is involved in CPX against cervical cancer cells.

3.2. CPX induces autophagosome accumulation in cervical cancer cells

Increasing evidence has highlighted the important role of autophagy in cancer treatment. To explore whether autophagy is regulated by CPX in cervical cancer cells, the conversion of MAP1LC3B/LC3BII was measured with CPX treatment. As shown in Fig. 2A–B and S2A-B, CPX treatment promoted the turnover of LC3B–I to lipidated LC3B-II in a dose- and time-dependent manner in HeLa and SiHa cells. The autophagic phenotype was further supported by the accumulation of autophagic vesicles (LC3B puncta) in CPX-treated cells compared with control cells (Fig. 2C–D). In addition, the transmission electron microscopy experiment also showed that autophagic lysosomes increased significantly in cervical cancer cells treated with CPX (Fig. 2E).

To explore whether the accumulated autophagosomes resulted from the activated autophagy, we used drugs and genetic tools to inhibit the induction of autophagy. Cells transfected with BECN1 or ATG5 siRNAs showed remarkably decreased LC3B lipidation and endogenous LC3B puncta accumulation even with CPX treatment (Fig. S2C-D). Consistently, co-administration of wortmannin, a PI3K inhibitor, also showed remarkably decreased of LC3B lipidation (Fig. S2E). Together, these findings reveal that CPX induces autophagy initiation in cervical cancer cells.

3.3. CPX promotes autophagy flux in cervical cancer cells

To further determine whether CPX induced complete autophagic flux, we first examined the protein levels of SQSTM1/p62, a well-known autophagic substrate. Decreased SQSTM1/p62 levels were observed in CPX-treated cells along with the increased LC3B-II levels (Figs. 2A and S2A). In addition, using a tandem monomeric RFP-GFP-tagged LC3B, we found that CPX treatment resulted in dramatic formation of red fluorescent autolysosomes, which transformed into yellow under co-

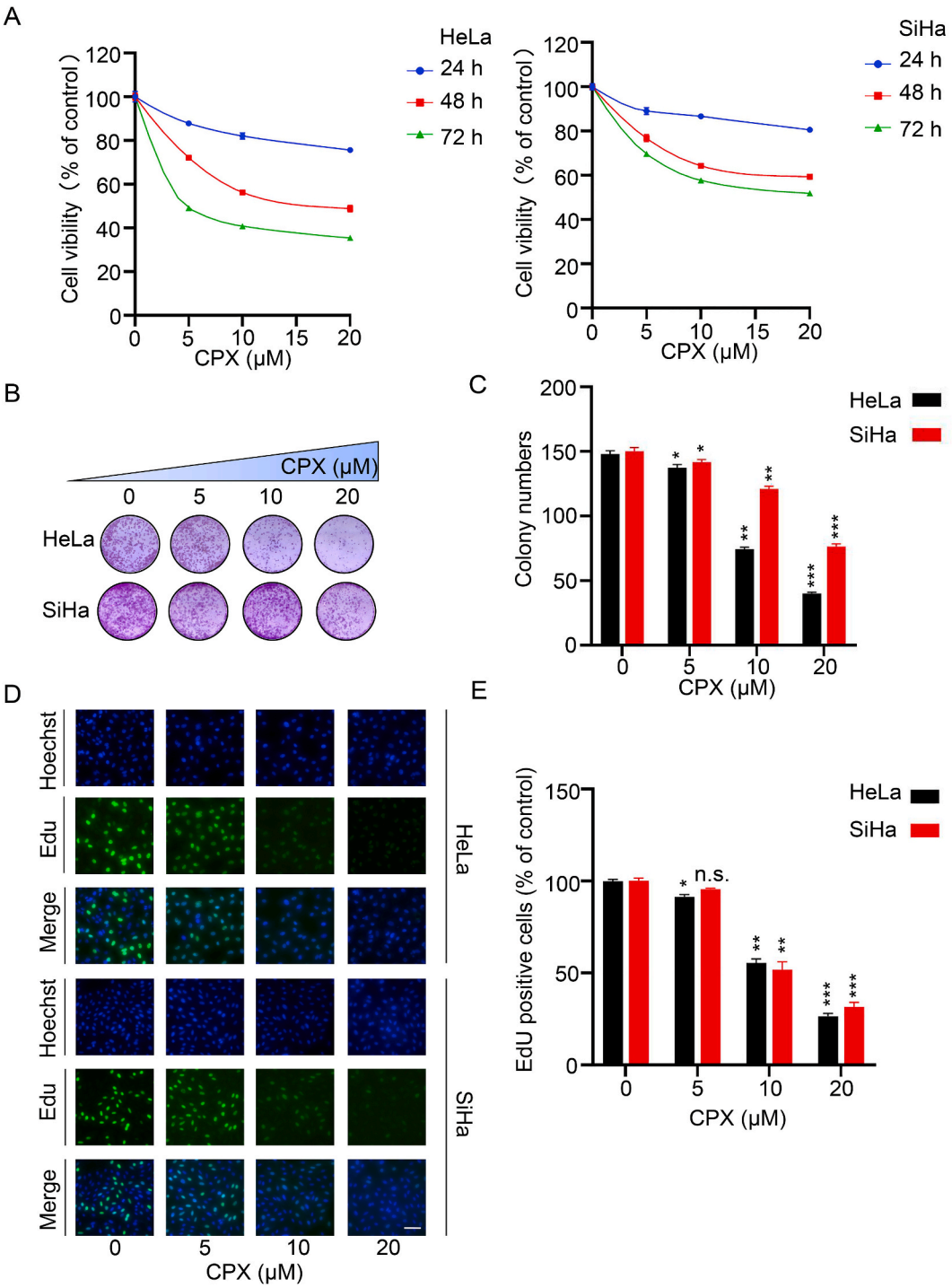

Fig. 1. CPX inhibits proliferation in cervical cancer cells

(**A**) HeLa and SiHa cells were treated with the indicated concentrations of CPX for 24 h, 48h, 72h and cell viability was determined by CCK8 kit. (**B** and **C**) Cell proliferation rate was analyzed by clone formation assay. HeLa and SiHa cells were treated with the indicated concentration of CPX for 24 h, after treatment, cells were seeded into 12-well plates for two weeks and colony numbers were quantified. (**D** and **E**) EdU assay of HeLa and SiHa cells treated with the indicated concentration of CPX for 24 h. The EdU incorporation was quantitated. Scale bar, 100 μm. Data are means ± s.d. and are representative of 3 independent experiments. *, $P < 0.05$, **, $P < 0.01$, ***, $P < 0.001$. Statistical significance compared with respective control groups.

treatment with CQ (Fig. 3A). To further confirm the fusion of autophagosomes with lysosomes in CPX-treated cells, we examined the colocalization between LC3B and LAMP1 (lysosome marker). CPX treatment induced obvious colocalization of LC3B with LAMP1, suggesting the fusion between autophagosomes and lysosomes was enhanced (Fig. 3B). We also used the autolysosome inhibitors (Baf A1, CQ, or E64D and Pepstatin A) to further assess the intact of autophagic flux and found that combinational treatment of CPX with autolysosome inhibitors resulted in further enhanced accumulation of LC3B-II (Fig. 3C–D and S3A-E). In summary, these results show that CPX induces complete autophagic flux in cervical cancer cells.

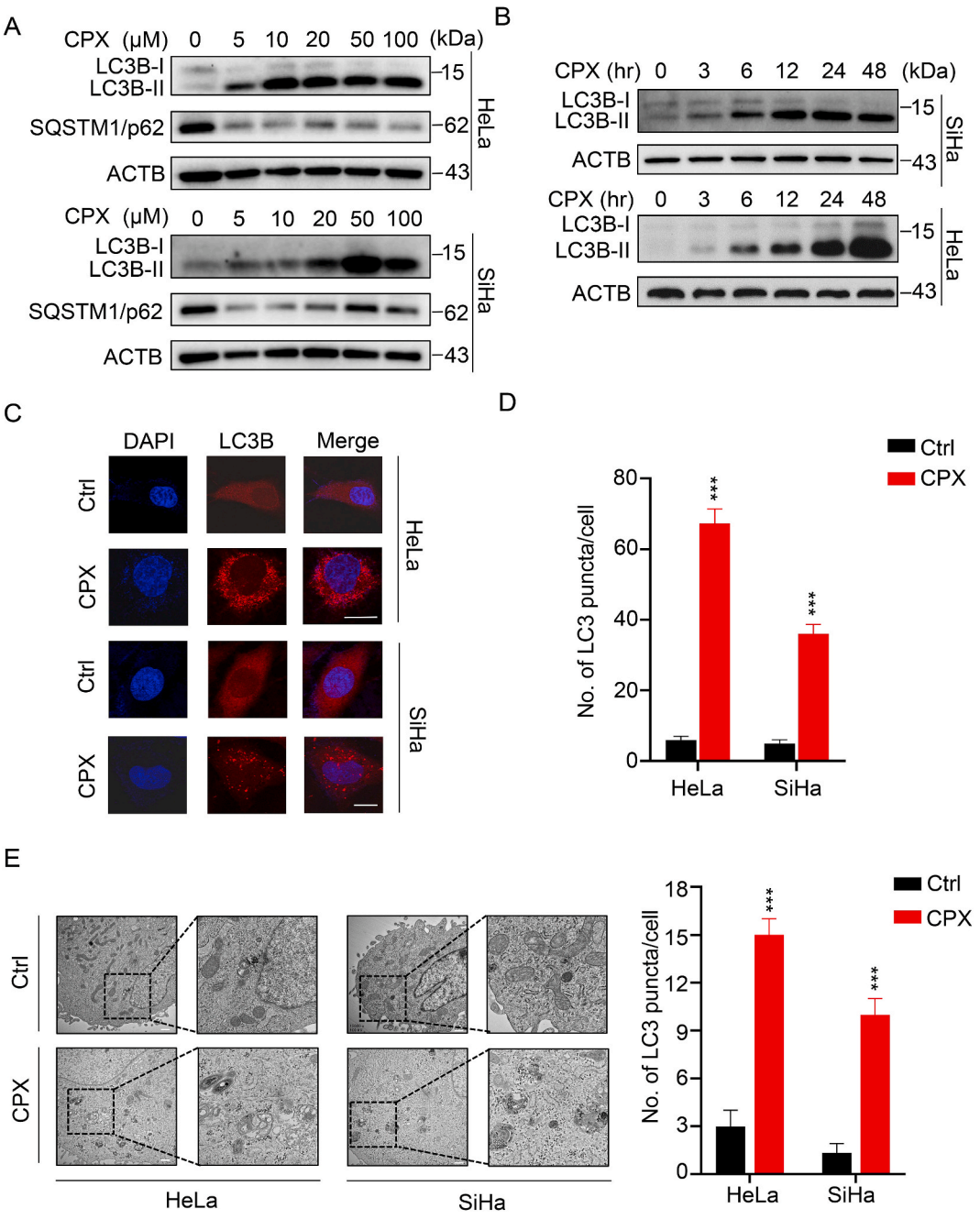

Fig. 2. CPX induces autophagosome accumulation in cervical cancer cells
(**A**) Immunoblot analysis of MAP1LC3B and SQSTM1/p62 expression in cervical cancer cells treated with the indicated concentrations of CPX for 24 h. (**B**) Time course analysis of MAP1LC3B expression in HeLa and SiHa cells treated with CPX (20 μM) for 3, 6, 12, 24, 48 h by immunoblotting. (**C and D**) The formation of endogenous LC3B puncta was shown and quantitated by immunofluorescence analysis in cells treated with or without 20 μM CPX for 24 h. Scale bar, 20 μm. (**E**) Autophagic vesicles were detected by transmission electron microscope in HeLa and SiHa cells treated with or without 20 μM CPX for 24 h. Scale bar, 1 μm. Data are means ± s.d. and are representative of 3 independent experiments. ***, $P < 0.001$. Statistical significance compared with respective control groups.

3.4. Autophagy attenuates CPX-induced anti-cancer effects

Considering that autophagy regulates the proliferation, migration and even chemo-sensitivity of cancer cells, we wondered whether the induction of autophagy by CPX affected its anti-cancer effects. HeLa and SiHa cells were treated with CPX combined with autophagy inhibitor CQ. Compared to CPX alone, combined treatment with CQ significantly decreased the cell viability of cervical cancer cells (Fig. 4A). A similar decrease in cell proliferation was also observed as evidenced by colony formation analysis and EdU labeling (Fig. 4B and C). In addition, LDH release assay revealed that CQ enhanced the cytotoxicity induced by CPX (Fig. 4D). We also found that CQ augmented CPX-induced apoptotic cell death, as evidenced by cleaved-PARP1 expression detected by western blotting (Fig. S4A). Accordingly, obvious cytoplasmic vacuole formation and morphological changes that are typical of apoptosis were observed in cells treated with CPX combined with CQ using the light microscope (Fig. 4E). In conclusion, these results suggest that autophagy attenuates the anti-cancer effects of CPX.

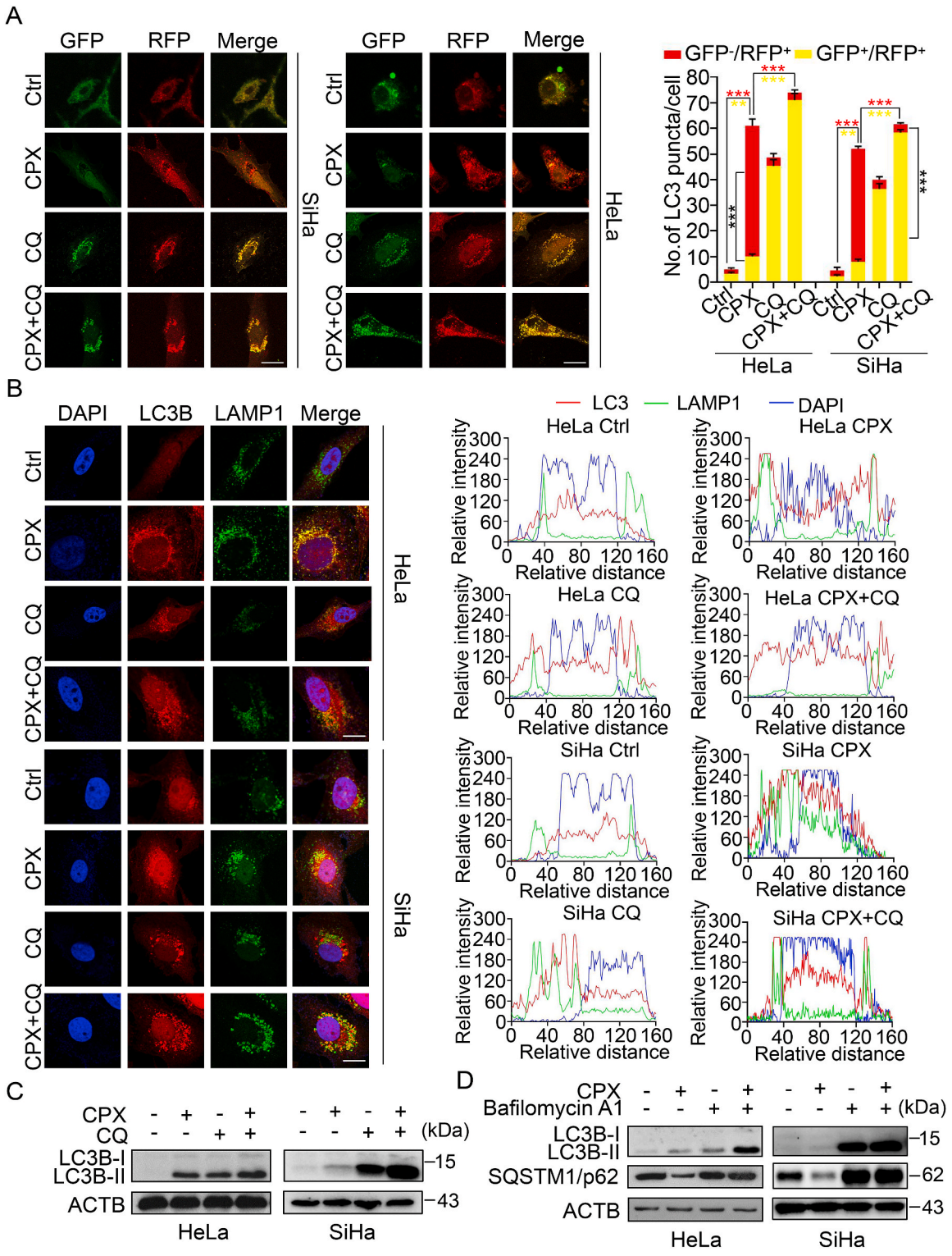

Fig. 3. CPX promotes autophagy flux in cervical cancer cells

(**A**) Immunofluorescence analysis of cells transiently transfected with tandem mRFP-GFP-tagged LC3B and treated with vehicle, CPX (20 μM), CQ (10 μM), or in combination for 24 h. Scale bar, 10 μm. The ratio of red puncta indicating autolysosomes (GFP-/RFP+) versus yellow puncta indicating autophagosomes (GFP+/RFP+) was quantitated. GFP: GFP-LC3B; RFP: RFP-LC3B. (**B**) Immunofluorescence analysis of the co-localization of endogenous LC3B and LAMP1 in cervical cancer cells treated with vehicle, CPX (20 μM), CQ (10 μM), or in combination for 24 h. Scale bar, 10 μm. (**C**) Cervical cancer cells were treated with vehicle, CPX (20 μM), CQ (10 μM), or in combination for 24 h. Immunoblot analysis was used to detect the expression of LC3B. (**D**) HeLa and SiHa cells were treated with CPX (20 μM) alone or in combination with Baf A1 (100 nM) for 24 h. The expressions of LC3B and SQSTM1/p62 were examined by immunoblotting. Data are means ± s.d. and are representative of 3 independent experiments. **, $P < 0.01$, ***, $P < 0.001$. Statistical significance compared with respective control groups. (For interpretation of the references to color in this figure legend, the reader is referred to the Web version of this article.)

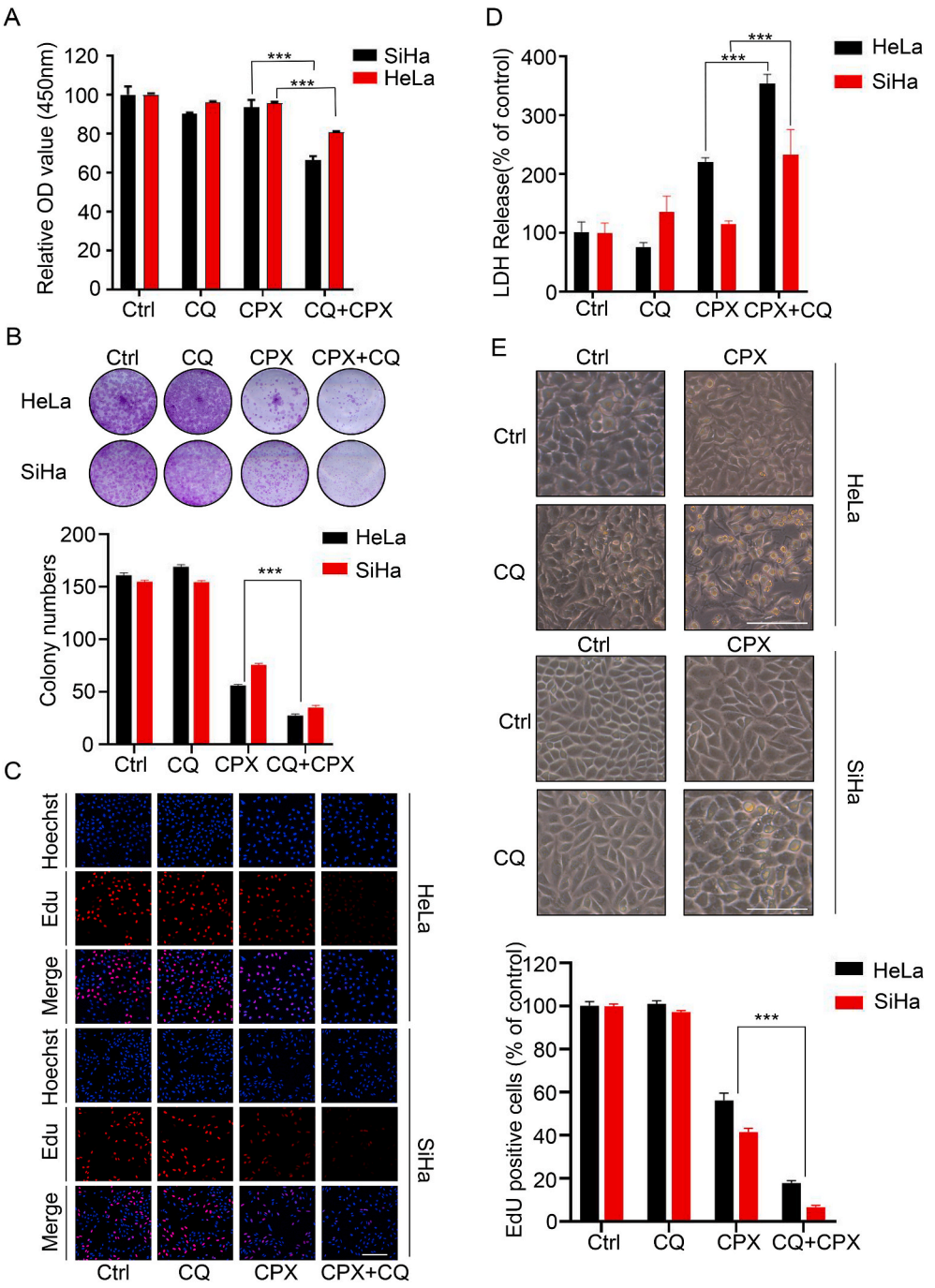

Fig. 4. Autophagy attenuates CPX-induced anti-cancer effects

Cervical cancer cells treated with 20 μM CPX in the presence or absence of 10 μM CQ for 24 h. (**A**) The cell viability was detected by CCK8 assays. (**B**) Cell proliferation was detected by colony formation assays. (**C**) The EdU incorporation was quantitated. Scale bar, 200 μm. (**D**) Analysis of the LDH release experiments. (**E**) Represented images of HeLa and SiHa cells following treatment. Scale bar, 50-μm. Data are means ± s.d. and are representative of 3 independent experiments. ***, $P < 0.001$. Statistical significance compared with respective control groups.

3.5. PARK7/PRKAA1/mTOR axis contributes to CPX-induced autophagy

Given that PRKAA1/mTOR pathway is the main regulator of autophagy induction, we next aimed to identify whether PRKAA1/mTOR pathway was involved in CPX-induced autophagy in cervical cancer cells. As shown as Fig. 5A and S5A, CPX treatment resulted in the activation of PRKAA1 and inhibition of mTOR, as demonstrated by increased phosphorylation levels of PRKAA1 and decreased phosphorylation levels of mTOR and RPS6KB1. Furthermore, inhibition of PRKAA1 with Compound C prominently inhibited CPX-induced elevation of LC3B lipidation (Fig. S6A). These results indicated that CPX activates autophagy by PRKAA1/mTOR pathway.

We have previously found that the expression of PARK7 was significantly reduced in CPX-treated colorectal cancer [5]. We supposed that PARK7 might be a target of CPX in the treatment of tumors. To determine whether PARK7 was involved in CPX-treated cervical cancer, we first detected the expression of PARK7. CPX treatment caused the decrease of PARK7 in a dose-dependent manner by transcriptional inhibition in HeLa and SiHa cells treated with CPX (Fig. 5B–C, S5B and S6B). We then evaluated the proliferation of cervical cancer cells stably overexpressing PARK7 under CPX treatment. As expected, PARK7 overexpression markedly reversed the inhibition of cell proliferation caused by CPX (Fig. 5D–E). We also detected the changes of autophagy and found that knocking down PARK7 could induce elevation of LC3B lipidation, however, CPX can further induce LC3B accumulation in PARK7 knockdown cells (Fig. S6C), suggesting in addition to PARK7, others molecules were also involved in CPX-induced autophagy. On the

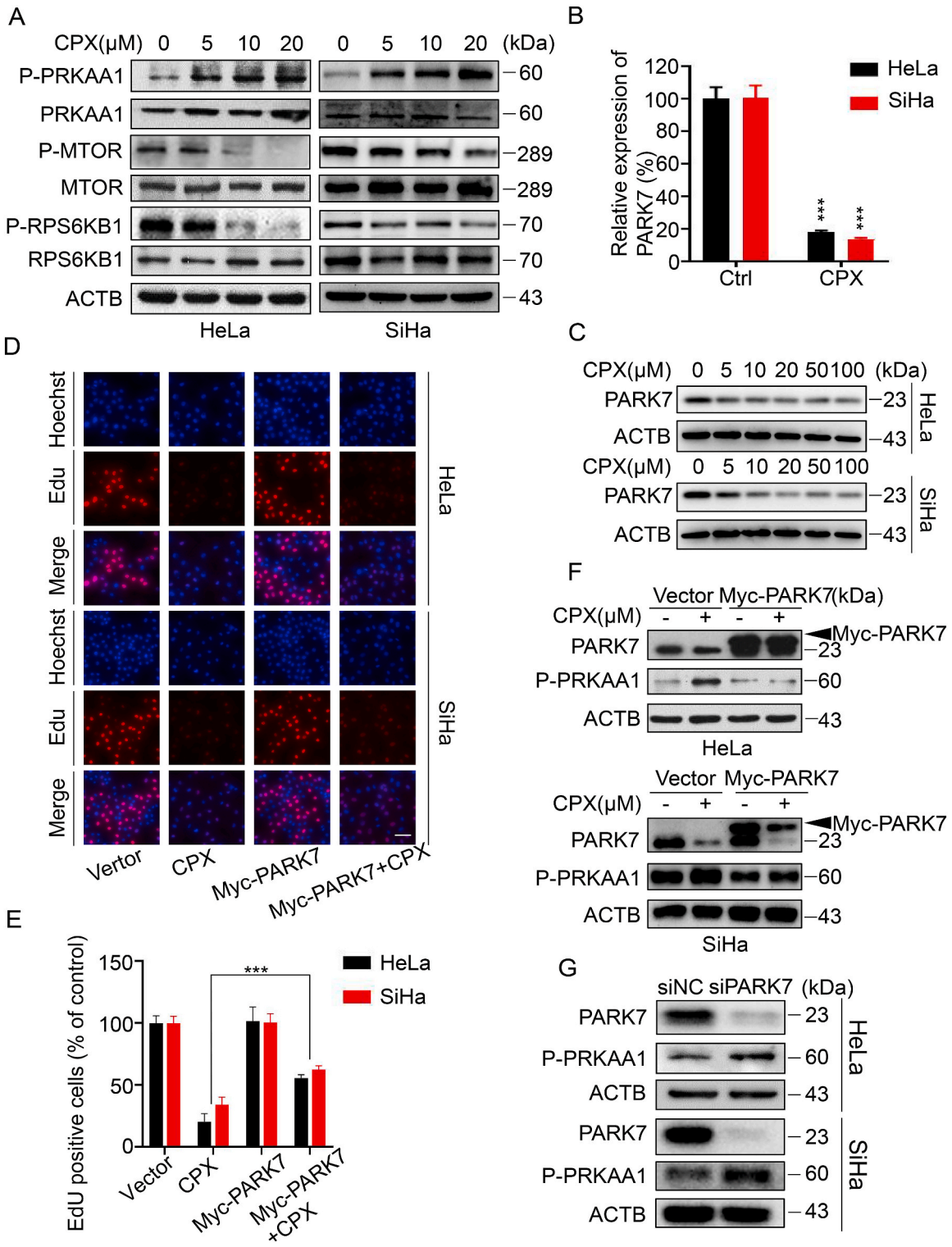

Fig. 5. PARK7/PRKAA1/MTOR axis contributes to CPX-induced autophagy

(**A**) Cervical cancer cells were treated with the indicated concentrations of CPX. The total and phosphorylation levels of PRKAA1, mTOR and RPS6KB1 were examined by immunoblotting. (**B**) qRT-PCR was conducted in HeLa and SiHa cells treated with or without 20 μM CPX for 24 h to determine the transcription of PARK7. (**C**) Immunoblot analysis of PARK7 expression in cervical cancer cells treated with or without the indicated concentration of CPX for 24 h. (**D** and **E**) EdU assays of HeLa and SiHa cells stably overexpressing PARK7 or Vector treated with or without 20 μM CPX for 24 h. The EdU incorporation was quantitated. Scale bar, 100 μm. (**F**) Immunoblot analysis on the expressions of PARK7 and phosphor-PRKAA1 in HeLa and SiHa cells transiently transfected with Vector or Myc-PARK7 plasmid for 24 h, followed by treatment with or without 20 μM CPX for another 24 h. (**G**) Immunoblot analysis on the protein levels of PARK7 and phosphor-PRKAA1 in cervical cancer cells transfected with siNC or siPARK7 for 24 h, followed by treatment with or without 20 μM CPX for another 24 h. Data are means ± s.d. and are representative of 3 independent experiments. ***, $P < 0.001$. Statistical significance compared with respective control groups.

contrary, PARK7 overexpression decreased CPX-induced LC3B-II levels in HeLa and SiHa cells (Fig. S6D).

Then we tested whether the activation of PRKAA1 is related to CPX-induced downregulation of PARK7. As shown as Fig. 5F–G and S5C-E, enforced exogenous expression of PARK7 in cervical cancer cells inhibited the activation of PRKAA1 and knockdown PARK7 induced its activation. Taken together, these findings suggest that CPX activates PRKAA1 and induces autophagy though downregulation of PARK7 in cervical cancer cells, at least in part.

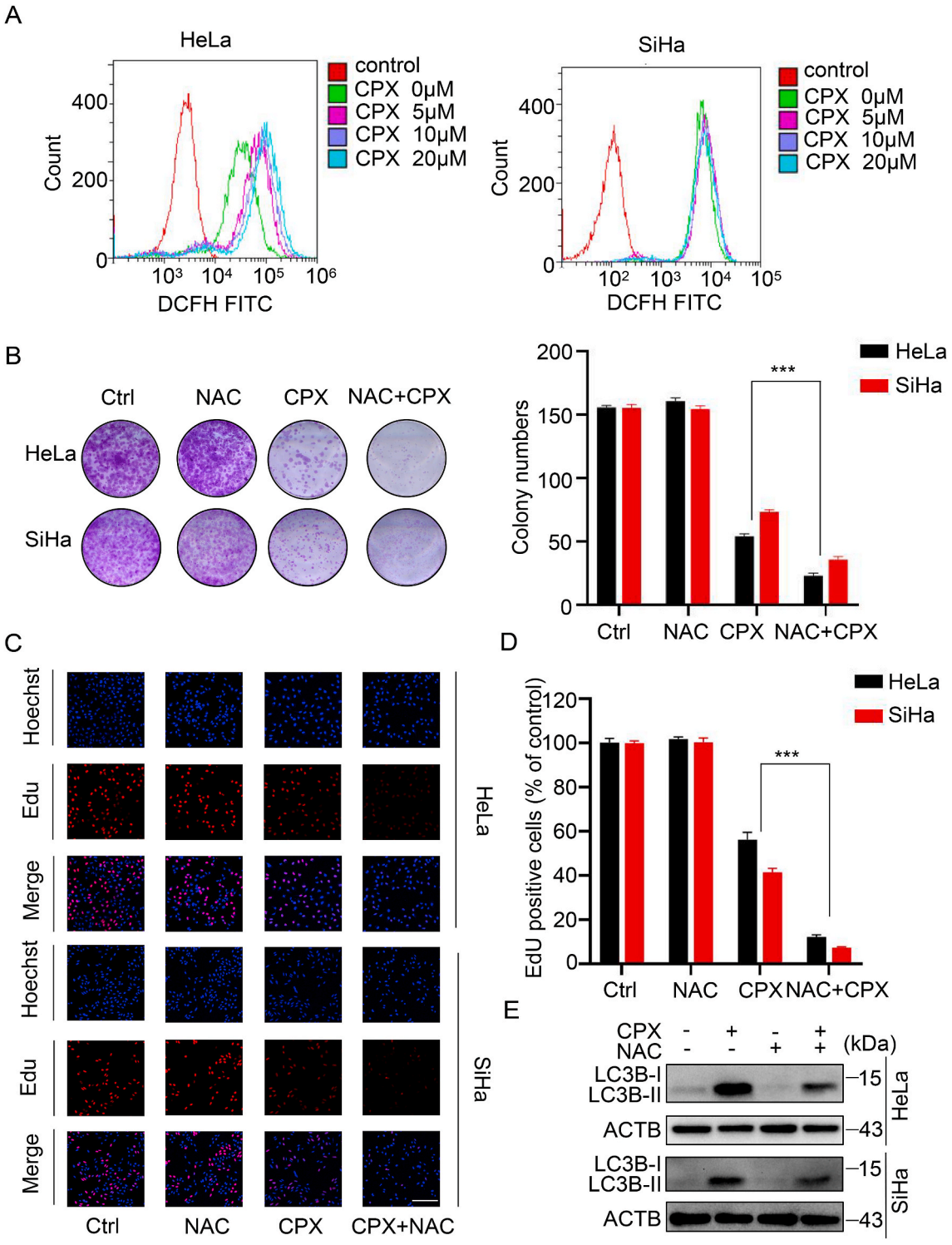

Fig. 6. ROS accumulation is essential for CPX-induced protective autophagy independent of PARK7

(**A**) ROS levels were determined by flow cytometry in cervical cancer cells treated with the indicated concentrations of CPX for 24 h. (**B**) HeLa and SiHa cells were treated with 20 μM CPX in the presence or absence of 5 mM NAC. Cell proliferation was detected by colony formation assays. (**C** and **D**) EdU assays of cervical cancer cells treated with 5 mM NAC in the presence or absence of 20 μM CPX for 24 h. The EdU incorporation was quantitated. Scale bar, 200 μm. (**E**) Immunoblot analysis of LC3B expression in HeLa and SiHa cells treated with CPX (20 μM) or vehicle and/or with NAC (5 mM). Data are means ± s.d. and are representative of 3 independent experiments. ***, $P < 0.001$. Statistical significance compared with respective control groups.

3.6. ROS accumulation is essential for CPX-induced protective autophagy independent of PARK7

Given the important role of PARK7 in regulating the redox balance which was usually involved in chemotherapy, we examined the levels of ROS by flow cytometry. CPX increased the levels of ROS in cervical cancer cells in a dose-dependent manner (Fig. 6A). Unexpectedly, PARK7 overexpression couldn't attenuate CPX-induced ROS accumulation in cervical cancer cells (Fig. S7A). To investigate the role of ROS in the anti-cancer effects induced by CPX, HeLa and SiHa cells were treated with CPX combined with NAC, ROS scavenger. Compared to CPX alone, combinational use with NAC significantly decreased the viability of cervical cancer cells (Fig. 6B–D and S7B–C). In addition, NAC treatment reduced LC3B-II turnover induced by CPX (Fig. 6E. and S7D), which might be achieved through the mTOR pathway, as evidenced by the increased phosphorylation level of MTOR (Fig. S7E). NAC even reduced CPX-induced the turnover of LC3B-II in the presence of the autolysosome inhibitor CQ (Fig. S7F), suggesting that ROS is essential for CPX-induced autophagy flux. Collectively, these results indicate that ROS accumulation is required for CPX-induced protective autophagy independent of PARK7 expression.

3.7. Glycophagy contributes to the anti-cancer effects of CPX

Interestingly, glycogen clustering and glycophagosomes formation were observed in CPX-treated HeLa and SiHa cells (Fig. 7A). While combinatorial treatment of CPX with the autolysosome inhibitor Baf A1 resulted in further clustering of glycogen in CPX-treated HeLa and SiHa cells (Fig. S8A), suggesting CPX may induce glycophagy in cervical cancer cells. Since STBD1 is exclusively employed to bind glycogen, and involved in the transport of glycogen to lysosomes by binding with GABARAPL1. Thus, the interaction between STBD1 and GABARAPL1 was further assessed. As shown in Fig. 7B, we found that CPX treatment increased the binding of STBD1 with GABARAPL1. In addition, co-localization analysis revealed that STBD1 strongly colocalized with GABARAPL1 in cervical cancer cells treated with CPX (Fig. 7C–D). These results indicated that CPX indeed could elicit glycophagy in cervical cancer cells. Thus, we wonder to reveal the role of glycophagy in CPX against cervical cancer cells. Quantitative analysis by Gene Expression Profiling Interactive Analysis confirmed the significant downregulation of STBD1 in cervical cancer relative to normal cervical tissues (Fig. S8B). Consistently, knockdown of STBD1 significantly reversed the inhibition of cell proliferation induced by CPX and enhanced the viability of CPX-treated cervical cancer cells (Fig. 7E and S8C-E). These findings indicate that glycophagy contributes to the anti-cancer effects of CPX.

Since we have demonstrated that CPX activated protective autophagy by downregulation of PARK7 and accumulation of ROS in the cervical cancer cells, we wondered whether PARK7 or ROS accounted for CPX-induced glycophagy. We first evaluated the glycogen clustering in cervical cancer cells stably overexpressing PARK7 under CPX treatment and found that the glycogen clustering remained unchanged with PARK7 overexpression (data not shown). The presence of NAC, however, led to the further clustering of glycogen in the cervical cancer cells treated with CPX (Fig. S8F), which might be caused by the reduction of autophagy (Fig. 6D). More interestingly, combinational use of NAC with CPX further enhanced the binding of STBD1 with GABARAPL1 in the cervical cancer cells (Fig. 7F). These results indicate that although the combinatorial treatment of CPX with NAC reduces the overall autophagy level in HeLa and SiHa cells, the lethal glycophagy is enhanced.

The synthesis and breakdown of glycogen is mainly accomplished by glycogen synthase (GYS1) and glycogen phosphorylase (PYGL). GSK3B can inactivate GYS1 by phosphorylation, thereby reducing glycogen synthesis. After knocking down GSK3B, glycogen clustering further increased in CPX-treated HeLa and SiHa cells (Fig. S8G). Consistently, knocking down GYS1 reduced glycogen clustering in cells treated with CPX (Fig. S9A). Besides, we found that GSK3B knockdown decreased while GYS1 knockdown increased the turnover of LC3B-II with CPX treatment (Fig. S9B-C). Furthermore, glycogen clustering was slightly reduced under starvation conditions in CPX-treated HeLa and SiHa cells (Fig. S9D). These results show that the upstream regulation of glycogen synthesis was also involved in the autophagy and the glycogen clustering induced by CPX in cervical cancer cells.

A recent report found that glycogen accumulation and phase separation block the activation of the Hippo signal and consequently activates YAP1, which promotes liver enlargement and cancer development [28]. We suspected whether CPX-mediated glycogen clustering would block phase separation of glycogen to regulate Hippo signaling activities. Therefore, we tested the activity of the YAP1 signaling pathway. As shown in Fig. S9E, CTGF and CYR61, target genes of YAP1, were downregulated upon CPX treatment, which was confirmed by the quantitative RT-PCR assay. In addition, the expression and nuclear localization of YAP1 were reduced in HeLa and SiHa cells treated with CPX (Fig. S9F-G). Together, these data indicate that CPX may inhibit the growth of cervical cancer cells by inhibiting the YAP1 pathway.

4. Discussion

CPX is a broad-spectrum fungicide, the effectiveness and safety of which have been well demonstrated [35,36]. Recent preclinical and clinical studies have shown that CPX also possesses promising anti-cancer activities [37–39]. It is of great significance to reveal the activity and mechanism of CPX in cancer therapy. In this study, we found that CPX exhibited remarkable anti-cancer effects on cervical cancer cells by inducing proliferation inhibition, which was achieved through downregulation of PARK7. Furthermore, CPX also caused the accumulation of ROS to elicit cytoprotective autophagy, decrease cellular glycogen clusters and inhibit glycophagy, which was independent of PARK7 expression. Therefore, autophagy and glycogen metabolisms may become used novel targets in overcoming the drug resistance of cervical cancer.

PARK7, a well-known oxidative stress sensor, mainly localized in the mitochondria and played a cytoprotective role by eliminating oxidative stress [40,41]. Several lines of evidence suggests that PARK7 is over-expressed in multiple types of tumors and is positively correlated with tumor progression, tumor recurrence, and chemotherapeutic drug resistance [42,43]. Arnouk et al. suggested that PARK7 is one of molecular markers for cervical carcinoma and the expression level is much higher than that in normal cervical tissues [44]. PARK7 contributes to the development of cervical cancer by improving the cell viability and inhibiting apoptosis [45]. A series of researches suggest that PARK7 can be used as a therapeutic target in the cancer treatment [42,46]. Suppressing the expression of PARK7 by diallyl disulfide (DADS) induces apoptosis and inhibits the metastatic potential of leukemia cells [47]. Our previous study found that CPX also targets PARK7 to inhibit the growth of colorectal cancer cells by inducing mitochondrial dysfunction and ROS accumulation [5]. In this study, we found that downregulation of PARK7 induced by CPX caused proliferation inhibition of cervical cancer cells. Therefore, PARK7 is an important anti-cancer target of CPX.

The roles of autophagy in response to chemotherapy is multifaceted [19]. On one hand, autophagy can be pro-death or inhibit proliferation to benefit the anti-cancer effects [48,49]. On the other hand, cytoprotective autophagy induced by therapeutic agents promotes cancer cell survival, leading to drug resistance [20,50]. In this study, we also found that CPX induced cytoprotective autophagy, resulted from PARK7-induced activation of PRKAA1 signaling. PARK7 is a traditional anti-oxidative protein and emerging evidence suggests that PARK7 may modulate autophagy dependent oxidative stress [51,52]. Ji Cao et al. found that in N-(4-hydroxyphenyl) retinamide (4-HPR)-treated HeLa cells, PARK7 acts as an intracellular redox sensor to detect the degree of ROS triggered by 4-HPR and determines the cellular response to 4-HPR by modifying its own oxidation status. Under mild oxidative stress, moderately oxidized PARK7 is recruited to ASK1 to inhibit its activity

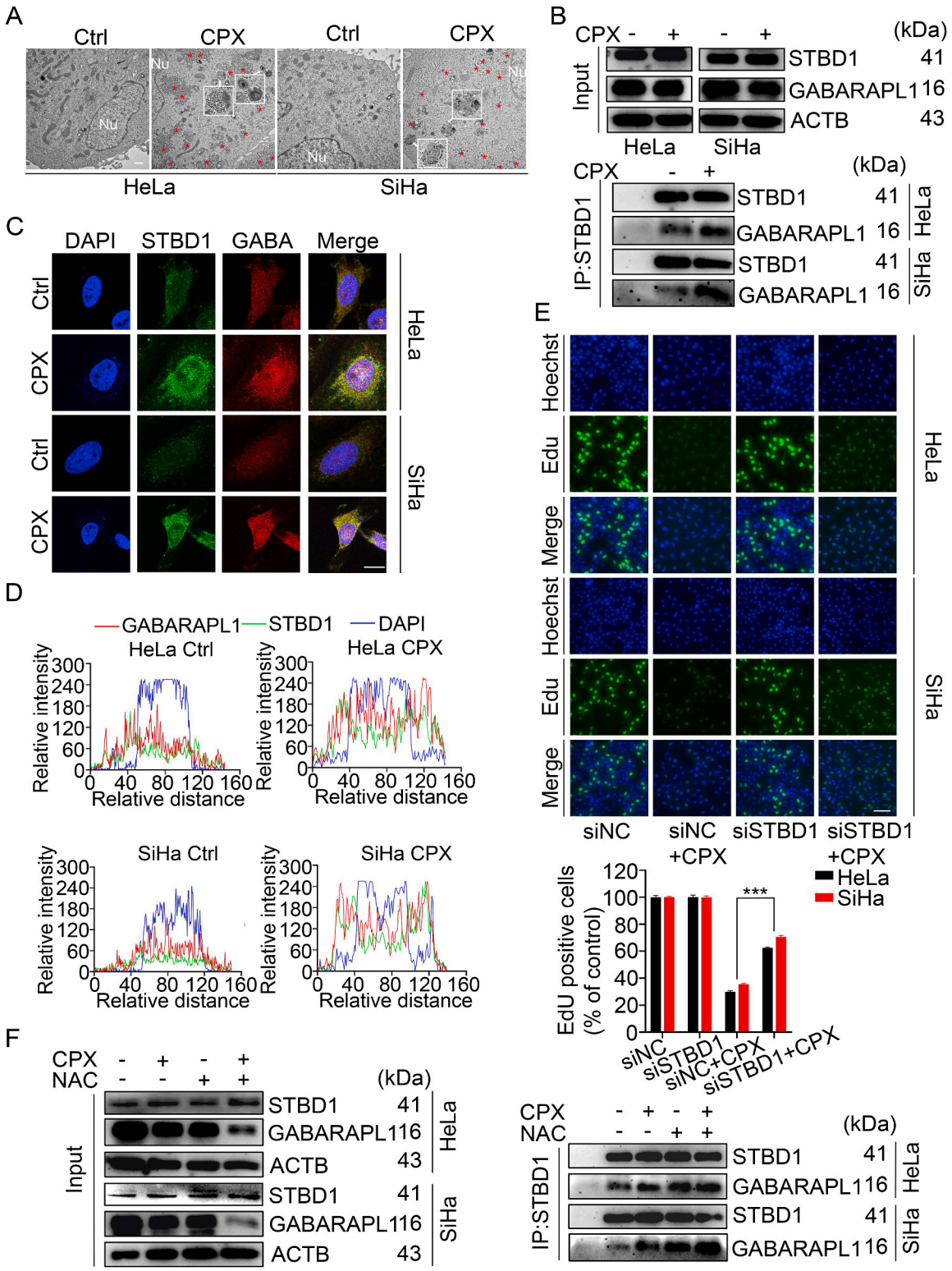

Fig. 7. Glycophagy contributes to the anti-cancer effects of CPX

(**A**) Aberrant subcellular glycogen deposits and glycophagosomes detected by transmission electron microscope in cervical cancer cells treated with or without 20 μM CPX for 24 h. The red asterisks indicate the glycogen clustering and the white arrows indicate glycophagosomes in the cytoplasm. Scale bar, 1 μm. (**B**) Co-immunoprecipitation assays were performed to determine the interaction between STBD1 and GABARAPL1 in cervical cancer cells treated with or without 20 μM CPX for 24 h. (**C** and **D**) Immunofluorescent images (**C**) and co-localization analysis (**D**) of STBD1 and GABARAPL1 to assess their co-localization in cervical cancer cells treated with or without 20 μM CPX for 24 h. Scale bar, 20 μm. GABA: GABARAPL1. (**E**) EdU assays of HeLa and SiHa cells transfected with siNC or siSTBD1 and treated with 20 μM CPX for 24 h. The EdU incorporation was quantitated. Scale bar, 100 μm. (**F**) The interaction between STBD1 and GABARAPL1 was determined by co-immunoprecipitation assays in cervical cancer cells treated with 20 μM CPX in the presence or absence of 5 mM NAC for 24 h. Data are means ± s. d. and are representative of 3 independent experiments. ***, $P < 0.001$. Statistical significance compared with respective control groups. (For interpretation of the references to color in this figure legend, the reader is referred to the Web version of this article.)

and keep the cell alive by activating autophagy [41]. In a previous study, we found CPX also targets PARK7 to trigger cell death and protective autophagy, which is dependent on ROS accumulation in colorectal cancer [5]. Zhou et al. found that CPX reduces cell viability and induces autophagy in human rhabdomyosarcoma cells which is attributed to the induction of ROS and ROS-mediated activation of the MAPK8 signaling pathway [53]. These studies suggest that PARK7 and ROS levels are essential for autophagy regulation. In addition, numerous chemotherapies are cytotoxic towards cancer cells by directly inducing drastic increases in ROS levels [54]. Interestingly, we found that CPX-induced ROS was protective rather than killing in cervical cancer cells and its protective effect was achieved by inhibiting MTOR to promote protective autophagy, which was independent of PARK7 expression. Therefore, we suppose that targeting ROS and autophagy in CPX-treated cervical cancer cells can promote the sensitivity of cervical cancer cells to CPX.

Decreased in glycogen content have been found in cervical carcinogenesis, causing the iodine test to be unstained [55]. Exfoliated cervical cancer cells from patients with poor responses to radiation or chemotherapy barely exhibit glycogen clustering in the cytoplasm. Therefore, glycogen clustering can be used as a sensitive indicator of cervical cancer treatment response and has prognostic value [29]. Cancer cells change glycogen storage and breakdown to sustain survival and growth according to the stages of cancer progression and tumor microenvironment [28]. Multiple studies have shown that glycogen is accumulated to improve several types of tumor cell survival under hypoxia or other stress conditions [29,56,57]. In addition, many human tumor cell lines derived from tissues that do not normally store glycogen have been shown to exhibit glycogen accumulation under stress [31]. Cancer cells rely primarily on aerobic glycolysis to sustain their proliferation, thus adapt glycogen catabolic pathway toward aerobic glycolysis was developed [58]. Inhibition of glycogen decomposition leads to reduced glucose oxidation, thereby delaying the growth of cancer cells [56,59]. In our study, CPX increased the clustering of glycogen in cervical cancer cells and combined use of NAC further promoted it, with enhanced inhibition of cell proliferation. Glycophagy is the glycogen breakdown pathway alternative to gluconeogenesis [28,31]. Inhibition of glycophagy may lead to metabolic reprogramming and thus promote tumorigenesis. STBD1 is the cargo receptor for glycogen autophagy, which is responsible for transporting glycogen into the lysosome to produce non-phosphorylated glucose [56,57]. Depletion of STBD1 or disruption its association with GABARAPL1 leads to enhanced glycolysis and accelerated growth in cancer cells, possibly through the pentose phosphate pathway. A recent study states that the W203C mutation of STBD1 impairs its co-localization with GABARAPL1 by disrupting its LIR motif, and inhibits the glycophagy and metabolic processes, thereby promoting tumor growth [20]. In this study, we found that CPX could promote glycophagy in cervical cancer cells. More interestingly, ROS scavenger inhibited CPX-induced autophagy whereas further enhanced lethal glycophagy, suggesting that ROS can attenuate the anti-cancer effects of CPX by inducing cytoprotective autophagy and simultaneously inhibiting glycophagy. Our study provides new evidence for the functional role of glycogen clustering and glycophagy in the treatment of cervical cancer and the selective regulation of autophagy in targeted cancers.

In addition, YAP1 plays a central role in controlling the progression of cervical cancer [60–62]. The expression of the master Hippo kinase MST1 was reduced in HPV positive cervical cell lines and cervical disease samples, leading to the activation of YAP1, thereby promoting cell proliferation [61]. The expression of YAP1 is associated with a poor prognosis for cervical cancer [63]. HPV E6 protein, a major etiological molecular of cervical cancer, maintains high YAP1 protein levels in cervical cancer cells by preventing the proteasome-dependent YAP1 degradation to drive the cervical cancer cell proliferation [61]. Meanwhile, a recent study revealed that accumulated glycogen undergoes liquid-liquid phase separation , which sequesters Hippo kinases MST1/2 in glycogen liquid droplets to relieve their inhibition on YAP1 [28]. In this study, we found that CPX induced the glycogen clustering and glycogen autophagy in cervical cancer cells, which possibly inhibits the dynamic changes of glycogen morphology and thereby affects the activation of Hippo. In accordance, CPX treatment significantly inhibited the activity of YAP1. These results suggest that inactivation of YAP1 was involved in CPX-induced proliferation inhibition in cervical cancer cells.

Collectively, our findings indicate that PARK7 is an important anticancer target of CPX and provide evidence for targeting cytoprotective autophagy as a potential chemotherapeutic strategy in cervical cancer. Our results also indicate that ROS-triggered glycophagy inhibition, glycogen clustering and glycogen clustering-mediated YAP1 inactivation may be used as new markers to monitor the therapeutic reactivity of cervical cancer.

Authors' contributions

Conception and design: Y. Lei; Acquisition of data (provided animals, acquired and managed patients, provided facilities, etc.): H. Fan, YJ. He, J. Zhou, JQ. Xiang, XY. Wan, JW. You, KL. Du; Analysis and interpretation of data (e.g., statistical analysis, biostatistics, computational analysis): Y. Lei, H. Fan, YJ. He, Y. Li, CD. Zhang, YT. Wang, Y. Bu; Writing, review, and/or revision of the manuscript: H. Fan, L. Cui, Y. Bu, Y. Lei; Study supervision: Y. Lei.

Declaration of competing interest

The authors declare that they have no known competing financial interests or personal relationships that could have appeared to influence the work reported in this paper.

Acknowledgements

This work was supported by grants from Chinese NSFC (81872014), Chongqing Natural Science Foundation (cstc2016jcyjA0227), CQMU Program for Youth Innovation in Future Medicine (W0089), and Chongqing Medical University Graduate Talent Training Program (BJRC202120).

Appendix A. Supplementary data

Supplementary data to this article can be found online at https://doi.org/10.1016/j.redox.2022.102339.

References

[1] H. Sung, et al., Global cancer statistics 2020: GLOBOCAN estimates of incidence and mortality worldwide for 36 cancers in 185 countries, CA A Cancer J. Clin. 71 (2021) 209–249, https://doi.org/10.3322/caac.21660.
[2] A. Buskwofie, G. David-West, C.A. Clare, A review of cervical cancer: incidence and disparities, J. Natl. Med. Assoc. 112 (2020) 229–232, https://doi.org/10.1016/j.jnma.2020.03.002.
[3] J. He, B. Huang, K. Zhang, M. Liu, T. Xu, Long non-coding RNA in cervical cancer: from biology to therapeutic opportunity, Biomed. Pharmacother. = Biomedecine & pharmacotherapie 127 (2020), 110209, https://doi.org/10.1016/j.biopha.2020.110209.
[4] J.A. Braun, et al., Effects of the antifungal agent ciclopirox in HPV-positive cancer cells: repression of viral E6/E7 oncogene expression and induction of senescence and apoptosis, Int. J. Cancer 146 (2020) 461–474, https://doi.org/10.1002/ijc.32709.
[5] J. Zhou, et al., CPX targeting DJ-1 triggers ROS-induced cell death and protective autophagy in colorectal cancer, Theranostics 9 (2019) 5577–5594, https://doi.org/10.7150/thno.34663.
[6] F. Al-Zubaydi, et al., Breast intraductal nanoformulations for treating ductal carcinoma in situ I: exploring metal-ion complexation to slow ciclopirox release, enhance mammary persistence and efficacy, J. Contr. Release : Off. j. Control. Release Soc. 323 (2020) 71–82, https://doi.org/10.1016/j.jconrel.2020.04.016.
[7] Z. Huang, S. Huang, Reposition of the fungicide ciclopirox for cancer treatment, Recent Pat. Anti-Cancer Drug Discov. 16 (2021) 122–135, https://doi.org/10.2174/1574892816666210211090845.

[8] M.D. Minden, et al., Oral ciclopirox olamine displays biological activity in a phase I study in patients with advanced hematologic malignancies, Am. J. Hematol. 89 (2014) 363–368, https://doi.org/10.1002/ajh.23640.

[9] N. Smith, M.A. Wilson, Structural biology of the DJ-1 superfamily, Adv. Exp. Med. Biol. 1037 (2017) 5–24, https://doi.org/10.1007/978-981-10-6583-5_2.

[10] B. Björkblom, et al., Reactive oxygen species-mediated DJ-1 monomerization modulates intracellular trafficking involving karyopherin β2, Mol. Cell Biol. 34 (2014) 3024–3040, https://doi.org/10.1128/mcb.00286-14.

[11] L.P. Dolgacheva, A.V. Berezhnov, E.I. Fedotova, V.P. Zinchenko, A.Y. Abramov, Role of DJ-1 in the mechanism of pathogenesis of Parkinson's disease, J. Bioenerg. Biomembr. 51 (2019) 175–188, https://doi.org/10.1007/s10863-019-09798-4.

[12] J. Cao, X. Chen, M. Ying, Q. He, B. Yang, DJ-1 as a therapeutic target against cancer, Adv. Exp. Med. Biol. 1037 (2017) 203–222, https://doi.org/10.1007/978-981-10-6583-5_13.

[13] W. Wang, et al., DJ-1 is a new prognostic marker and predicts chemotherapy efficacy in colorectal cancer, Oncol. Rep. 44 (2020) 77–90, https://doi.org/10.3892/or.2020.7593.

[14] B. Qiu, et al., DJ-1 promotes development of DEN-induced hepatocellular carcinoma and proliferation of liver cancer cells, Oncotarget 8 (2017) 8499–8511, https://doi.org/10.18632/oncotarget.14293.

[15] X.Y. He, et al., Serum DJ-1 as a diagnostic marker and prognostic factor for pancreatic cancer, J. Dig. Dis. 12 (2011) 131–137, https://doi.org/10.1111/j.1751-2980.2011.00488.x.

[16] H. Folkerts, S. Hilgendorf, E. Vellenga, E. Bremer, V.R. Wiersma, The multifaceted role of autophagy in cancer and the microenvironment, Med. Res. Rev. 39 (2019) 517–560, https://doi.org/10.1002/med.21531.

[17] Y. Kondo, T. Kanzawa, R. Sawaya, S. Kondo, The role of autophagy in cancer development and response to therapy, Nat. Rev. Cancer 5 (2005) 726–734, https://doi.org/10.1038/nrc1692.

[18] E. Wirawan, T. Vanden Berghe, S. Lippens, P. Agostinis, P. Vandenabeele, Autophagy: for better or for worse, Cell Res. 22 (2012) 43–61, https://doi.org/10.1038/cr.2011.152.

[19] D.A. Gewirtz, The four faces of autophagy: implications for cancer therapy, Cancer Res. 74 (2014) 647–651, https://doi.org/10.1158/0008-5472.Can-13-2966.

[20] L. Liu, et al., HMGB1-induced autophagy promotes chemotherapy resistance in leukemia cells, Leukemia 25 (2011) 23–31, https://doi.org/10.1038/leu.2010.225.

[21] P. Auberger, A. Puissant, Autophagy, a key mechanism of oncogenesis and resistance in leukemia, Blood 129 (2017) 547–552, https://doi.org/10.1182/blood-2016-07-692707.

[22] C. Kraft, F. Reggiori, M. Peter, Selective types of autophagy in yeast, Biochim. Biophys. Acta 1793 (2009) 1404–1412, https://doi.org/10.1016/j.bbamcr.2009.02.006.

[23] Han, Z. et al. Model-based analysis uncovers mutations altering autophagy selectivity in human cancer. Nat. Commun. 12, 3258, doi:10.1038/s41467-021-23539-5(2021).

[24] M.M. Adeva-Andany, M. González-Lucán, C. Donapetry-García, C. Fernández-Fernández, E. Ameneiros-Rodríguez, Glycogen metabolism in humans, BBA Clin. 5 (2016) 85–100, https://doi.org/10.1016/j.bbacli.2016.02.001.

[25] R. Resaz, et al., Development of hepatocellular adenomas and carcinomas in mice with liver-specific G6Pase-α deficiency, Dis. Model. Mech. 7 (2014) 1083–1091, https://doi.org/10.1242/dmm.014878.

[26] L.H. Wilson, et al., Liver glycogen phosphorylase deficiency leads to profibrogenic phenotype in a murine model of glycogen storage disease type VI, Hepatol. Commun. 3 (2019) 1544–1555, https://doi.org/10.1002/hep4.1426.

[27] P. Dauer, E. Lengyel, New roles for glycogen in tumor progression, Trends in cancer 5 (2019) 396–399, https://doi.org/10.1016/j.trecan.2019.05.003.

[28] Q. Liu, et al., Glycogen accumulation and phase separation drives liver tumor initiation, Cell 184 (2021) 5559–5576, https://doi.org/10.1016/j.cell.2021.10.001, e5519.

[29] M. Curtis, et al., Fibroblasts mobilize tumor cell glycogen to promote proliferation and metastasis, Cell Metabol. 29 (2019) 141–155, https://doi.org/10.1016/j.cmet.2018.08.007, e149.

[30] C. Ritterson Lew, S. Guin, D. Theodorescu, Targeting glycogen metabolism in bladder cancer, Nat. Rev. Urol. 12 (2015) 383–391, https://doi.org/10.1038/nrurol.2015.111.

[31] C.E. Zois, A.L. Harris, Glycogen metabolism has a key role in the cancer microenvironment and provides new targets for cancer therapy, J. Mol. Med. (Berl. Ger) 94 (2016) 137–154, https://doi.org/10.1007/s00109-015-1377-9.

[32] D.K. Das, J.R. Chowdury, The use of glycogen studies in the evaluation of treatment for carcinoma of the cervix uteri, Acta Cytol. 25 (1981) 566–571.

[33] J. Zhou, et al., DJ-1 promotes colorectal cancer progression through activating PLAGL2/Wnt/BMP4 axis, Cell Death Dis. 9 (2018) 865, https://doi.org/10.1038/s41419-018-0883-4.

[34] N. Xie, et al., PRKAA/AMPK restricts HBV replication through promotion of autophagic degradation, Autophagy 12 (2016) 1507–1520, https://doi.org/10.1080/15548627.2016.1191857.

[35] C. Mihailidou, P. Papakotoulas, A.G. Papavassiliou, M.V. Karamouzis, Superior efficacy of the antifungal agent ciclopirox olamine over gemcitabine in pancreatic cancer models, Oncotarget 9 (2018) 10360–10374, https://doi.org/10.18632/oncotarget.23164.

[36] K.M. Bernier, L.A. Morrison, Antifungal drug ciclopirox olamine reduces HSV-1 replication and disease in mice, Antivir. Res. 156 (2018) 102–106, https://doi.org/10.1016/j.antiviral.2018.06.010.

[37] P.M. Clement, H.M. Hanauske-Abel, E.C. Wolff, H.K. Kleinman, M.H. Park, The antifungal drug ciclopirox inhibits deoxyhypusine and proline hydroxylation, endothelial cell growth and angiogenesis in vitro, Int. J. Cancer 100 (2002) 491–498, https://doi.org/10.1002/ijc.10515.

[38] T. Shen, et al., Ciclopirox inhibits cancer cell proliferation by suppression of Cdc25A, Genes & cancer 8 (2017) 505–516, https://doi.org/10.18632/genesandcancer.135.

[39] J. Wu, et al., Antileukemia effect of ciclopirox olamine is mediated by downregulation of intracellular ferritin and inhibition β-Catenin-c-Myc signaling pathway in glucocorticoid resistant T-ALL cell lines, PLoS One 11 (2016), e0161509, https://doi.org/10.1371/journal.pone.0161509.

[40] C.M. Clements, R.S. McNally, B.J. Conti, T.W. Mak, J.P. Ting, DJ-1, a cancer- and Parkinson's disease-associated protein, stabilizes the antioxidant transcriptional master regulator Nrf2, Proc. Natl. Acad. Sci. U.S.A. 103 (2006) 15091–15096, https://doi.org/10.1073/pnas.0607260103.

[41] J. Cao, et al., The oxidation states of DJ-1 dictate the cell fate in response to oxidative stress triggered by 4-hpr: autophagy or apoptosis? Antioxidants Redox Signal. 21 (2014) 1443–1459, https://doi.org/10.1089/ars.2013.5446.

[42] J. Cao, S. Lou, M. Ying, B. Yang, DJ-1 as a human oncogene and potential therapeutic target, Biochem. Pharmacol. 93 (2015) 241–250, https://doi.org/10.1016/j.bcp.2014.11.012.

[43] W. Jin, Novel insights into PARK7 (DJ-1), a potential anti-cancer therapeutic target, and implications for cancer progression, J. Clin. Med. 9 (2020), https://doi.org/10.3390/jcm9051256.

[44] H. Arnouk, et al., Characterization of molecular markers indicative of cervical cancer progression, Proteonomics Clin. Appl. 3 (2009) 516–527, https://doi.org/10.1002/prca.200800068.

[45] H. Wang, W. Gao, DJ-1 expression in cervical carcinoma and its effects on cell viability and apoptosis, Med. Sci. Mon. Int. Med. J. Exp. Clin. Res. : Intern. Med. J. Exp. Clin. Res. 22 (2016) 2943–2949, https://doi.org/10.12659/msm.896861.

[46] Kim, J. Y. et al. PARK7 maintains the stemness of glioblastoma stem cells by stabilizing epidermal growth factor receptor variant III. Oncogene 40, 508-521, doi:10.1038/s41388-020-01543-1(2021).

[47] Q. Li, et al., Subcellular localization of DJ-1 in human HL-60 leukemia cells in response to diallyl disulfide treatment, Mol. Med. Rep. 14 (2016) 4666–4672, https://doi.org/10.3892/mmr.2016.5831.

[48] J. Yan, et al., Tubeimoside-I sensitizes colorectal cancer cells to chemotherapy by inducing ROS-mediated impaired autophagolysosomes accumulation, J. Exp. Clin. Cancer Res. : CR (Clim. Res.) 38 (2019) 353, https://doi.org/10.1186/s13046-019-1355-0.

[49] J.M.M. Levy, C.G. Towers, A. Thorburn, Targeting autophagy in cancer, Nat. Rev. Cancer 17 (2017) 528–542, https://doi.org/10.1038/nrc.2017.53.

[50] Z.J. Yang, C.E. Chee, S. Huang, F.A. Sinicrope, The role of autophagy in cancer: therapeutic implications, Mol. Cancer Therapeut. 10 (2011) 1533–1541, https://doi.org/10.1158/1535-7163.Mct-11-0047.

[51] M.K. McCoy, M.R. Cookson, DJ-1 regulation of mitochondrial function and autophagy through oxidative stress, Autophagy 7 (2011) 531–532, https://doi.org/10.4161/auto.7.5.14684.

[52] G. Krebiehl, et al., Reduced basal autophagy and impaired mitochondrial dynamics due to loss of Parkinson's disease-associated protein DJ-1, PLoS One 5 (2010), e9367, https://doi.org/10.1371/journal.pone.0009367.

[53] H. Zhou, et al., Ciclopirox induces autophagy through reactive oxygen species-mediated activation of JNK signaling pathway, Oncotarget 5 (2014) 10140–10150, https://doi.org/10.18632/oncotarget.2471.

[54] S. Galadari, A. Rahman, S. Pallichankandy, F. Thayyullathil, Reactive oxygen species and cancer paradox: to promote or to suppress? Free Radic. Biol. Med. 104 (2017) 144–164, https://doi.org/10.1016/j.freeradbiomed.2017.01.004.

[55] Reich, O. & Pickel, H. 100 years of iodine testing of the cervix: a critical review and implications for the future. Eur. J. Obstet. Gynecol. Reprod. Biol. 261, 34-40, doi:10.1016/j.ejogrb.2021.04.011(2021).

[56] E. Favaro, et al., Glucose utilization via glycogen phosphorylase sustains proliferation and prevents premature senescence in cancer cells, Cell Metabol. 16 (2012) 751–764, https://doi.org/10.1016/j.cmet.2012.10.017.

[57] J. Pelletier, et al., Glycogen synthesis is induced in hypoxia by the hypoxia-inducible factor and promotes cancer cell survival, Front. Oncol. 2 (2012) 18, https://doi.org/10.3389/fonc.2012.00018.

[58] S.Y. Lunt, M.G. Vander Heiden, Aerobic glycolysis: meeting the metabolic requirements of cell proliferation, Annu. Rev. Cell Dev. Biol. 27 (2011) 441–464, https://doi.org/10.1146/annurev-cellbio-092910-154237.

[59] W.N. Lee, et al., Metabolic sensitivity of pancreatic tumour cell apoptosis to glycogen phosphorylase inhibitor treatment, Br. J. Cancer 91 (2004) 2094–2100, https://doi.org/10.1038/sj.bjc.6602243.

[60] J.S. Mo, H.W. Park, K.L. Guan, The Hippo signaling pathway in stem cell biology and cancer, EMBO Rep. 15 (2014) 642–656, https://doi.org/10.15252/embr.201438638.

[61] C. He, et al., The Hippo/YAP pathway interacts with EGFR signaling and HPV oncoproteins to regulate cervical cancer progression, EMBO Mol. Med. 7 (2015) 1426–1449, https://doi.org/10.15252/emmm.201404976.

[62] H. Xiao, et al., Expression of Yes-associated protein in cervical squamous epithelium lesions, Int. J. Gynecol. Cancer : Off. J. Intern. Gynecol. Cancer Soc. 24 (2014) 1575–1582, https://doi.org/10.1097/igc.0000000000000259.

[63] C.A. Hall, et al., Hippo pathway effector Yap is an ovarian cancer oncogene, Cancer Res. 70 (2010) 8517–8525, https://doi.org/10.1158/0008-5472.Can-10-1242.